WDM Switching Employing a Hybrid Silicon-Plasmonic A-MZI

S. Papaioannou[(1),(2)], G. Giannoulis[(3)], D. Kalavrouziotis[(3)], K. Vyrsokinos[(2)], J.-C. Weeber[(4)], K. Hassan[(4)], L. Markey[(4)], A. Dereux[(4)], A. Kumar[(5)], S. I. Bozhevolnyi[(5)], D. Apostolopoulos[(3)], H. Avramopoulos[(3)], N. Pleros[(1),(2)]

[(1)] Department of Informatics, Aristotle University of Thessaloniki, Greece, sopa@csd.auth.gr
[(2)] Informatics & Telematics Institute, Center for Research & Technology Hellas, Thessaloniki, Greece
[(3)] School of Electrical & Computer Engineering, National Technical University of Athens, Greece
[(4)] Institut Carnot de Bourgogne, University of Burgundy, Dijon, France
[(5)] Institute of Technology and Innovation, University of Southern Denmark, Odense, Denmark

Abstract *We demonstrate a system-level evaluation of an A-MZI with 60µm long DLSPP active branches exhibiting more than 14dB extinction ratio. Error-free switching operation is achieved for a 4×10Gb/s incoming WDM data stream with only 13.1mW power consumption.*

Introduction

The emerging necessity for high-throughput, low-power and small-footprint circuits in the rapidly growing High Performance Computing Systems has drawn the attention to the development of next-generation chip-scale optical interconnects. In this perspective, plasmonics appears as a "beyond Silicon Photonics" [1] promising candidate for implementing low-power and small-footprint active functional devices. The propagation of Surface Plasmon Polariton (SPP) waves along metallic stripes yields strong mode confinements even at sub-wavelength scale, while the underlying metallic circuitry enables an inherently and seamless energy-efficient mechanism for the interplay between light beams and electrical control signals.

Dielectric Loaded SPP (DLSPP) waveguides offer enhanced power savings by using a dielectric polymer material on top of the metallic film and their potential to yield low footprint and highly functional low power on-chip circuitry has been demonstrated in many implementations such as thermo-optic (TO) modulation [2], On/Off gating [3] and switching [4], greatly benefiting also from their recent successful interfacing with the low-loss silicon photonic waveguide transmission platform [5].

TO tuning of Polymethylmethacrylate (PMMA)-loaded SPP -based racetrack resonators has been recently demonstrated by us in [5] with only 3.3mW power consumption providing the first solid proof of the low power characteristics of the DLSPP platform. The compatibility of DLSPP switches with true data carrying environments has been presented in [3] with an active PMMA-loaded SPP-based Asymmetric Mach Zehnder Interferometer (A-MZI) comprising 90µm plasmonic phase arms, through a single-channel 10Gb/s optical data

traffic switching operation. However photonic Network-on-Chip (NoC) implementations require compatibility with WDM technology towards increasing the aggregate on-chip throughput and facilitating the adoption of legacy concepts from telecom networks such as wavelength routing.

In this work, we introduce active plasmonics into WDM switching applications, using the smallest ever reported TO PMMA-loaded SPP switch based on an A-MZI with only 60µm long active phase branches. Error-free performance was attained for 4×10Gb/s data carrying channels with the maximum power penalty measured 3.6dB for a Bit Error Rate (BER) of 10^{-9}, while consuming only 13.1mW. The obtained results demonstrate the compatibility of active plasmonics with WDM technology concepts, verifying their combinational applicability in NoC environments.

Experimental setup

The A-MZI presented in this work is similar to the one used in [3], incorporating 60µm-long active plasmonic branches and exhibiting TO time constants lying in the 3-5µs area. By applying a Direct Current (DC) up to 40mA at its upper branch, static Extinction Ratio (ER) values of 14dB and 0.9dB for the CROSS and BAR ports, respectively, have been measured (Fig. 1(a)). The poor ER value for the BAR port stemmed from the 95:5, instead of 50:50, silicon input/output couplers employed at the MZI, due to an unfortunate design error that prevented the realization of a high performance 2×2 switch. The experimental setup used for the WDM switching application is shown in Fig. 1(b). Four continuous wave (CW) laser sources emitting light at 1545.1nm, 1546.7nm, 1547.7nm and 1549.1nm were multiplexed in pairs and each channel pair was modulated to a 10Gb/s 2^{31}-1 Non-Return-to-Zero (NRZ) data signal by a
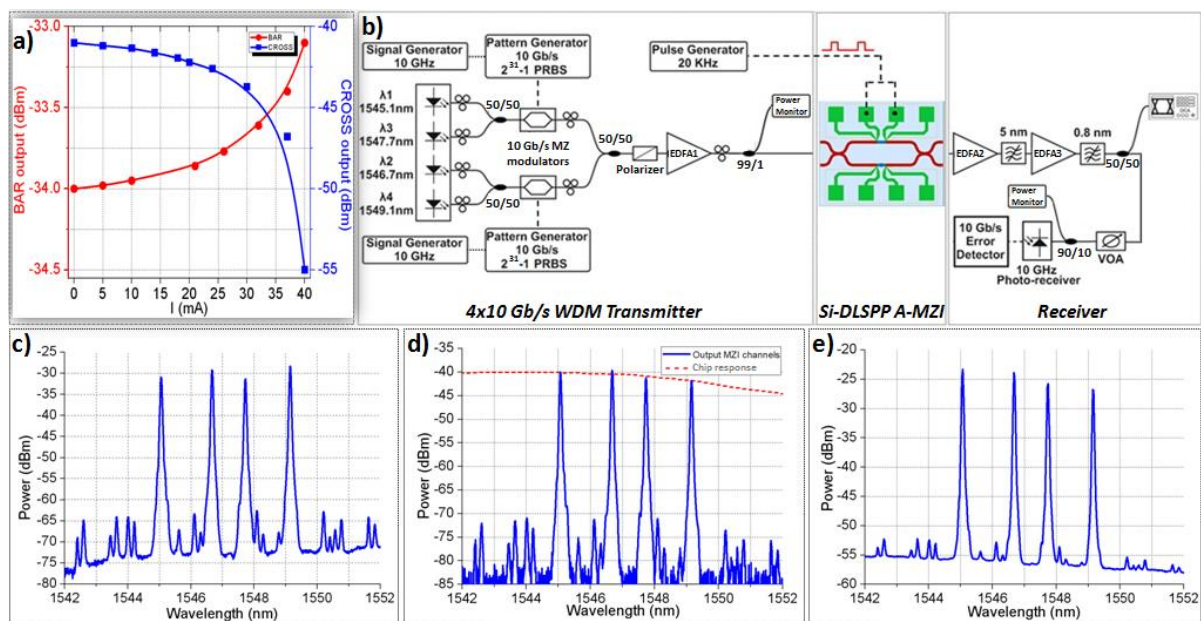
Fig. 1: (a) Static thermo-optic (TO) transfer functions for the CROSS and BAR output ports of the A-MZI, (b) Experimental setup and the 4-channel spectrum at (c) MZI input, (d) directly at the MZI output before entering EDFA2, (e) after the receiver's pre-amplification stage. The spectral response of the chip including the A-MZI and the TM grating couplers is shown with the red dashed line in (d).

corresponding Ti:LiNbO$_3$ Mach-Zehnder modulator. The four data streams were multiplexed into a 4×10Gb/s WDM signal that was then amplified by a high-power Erbium Doped Fiber Amplifier (EDFA) providing 31dBm power at the input of the electrically controlled DLSPP-based A-MZI. After exiting the A-MZI, the WDM data signal was amplified in a two stage EDFA with a 5nm midstage optical bandpass filter (OBPF) for out-of-band Amplified Spontaneous Emission (ASE) noise rejection. Individual channel isolation was performed after EDFA3 with a 0.8nm OBPF and the signal quality was evaluated by means of a sampling oscilloscope and a photo-receiver followed by an error-detector.

Fig. 1(c) illustrates the 4-channel spectrum after being amplified by EDFA1 and prior entering the A-MZI. The unequal power profile of the WDM signal owes mainly to the respective non-flattened gain profile of the high-power

EDFA1 as well as to the energy transfer to the four-wave mixing (FWM) terms that originate as a result of the high-power signal propagating in the fiber link between EDFA1 and the A-MZI. The FWM components within the 1545-1549nm wavelength window are, however, out-of-band with respect to the data channels so that they can be easily isolated by subsequent filtering stages. Fig. 1(d) shows the corresponding 4-channel spectrum directly at the output of the A-MZI, revealing that its spectral power profile has been altered compared to the corresponding A-MZI input profile and follows the power distribution dictated by the A-MZI's spectral response including the TM grating couplers, also depicted in this figure by the dashed line. As can be noticed, the spectral response of the chip over the wavelength window of interest has a clear wavelength-dependent behavior with the transmission losses increasing by 3dB when moving from 1545nm to 1550nm, originating
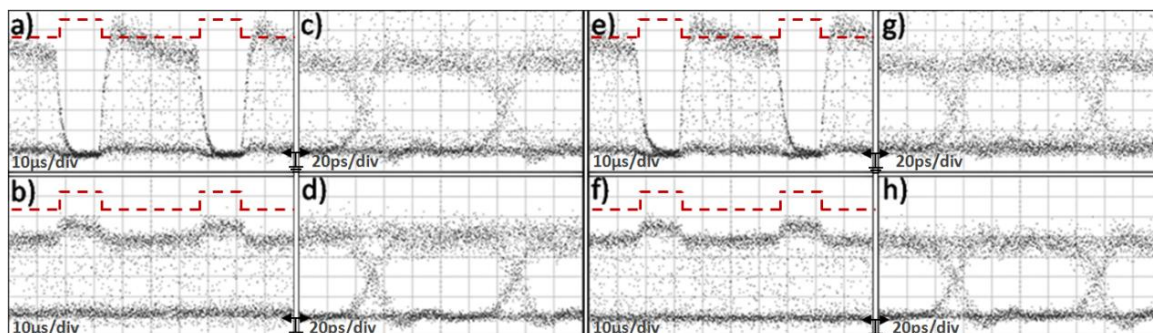

Fig. 2: Modulation with 15µs electrical rectangular pulses at 20KHz repetition rate for 10Gb/s (a) data trace at the CROSS port (channel 1), (b) data trace at the BAR port (channel 1), (c) eye diagram at the CROSS port (channel 1), (d) eye diagram at the BAR port (channel 1), (e) data trace at the CROSS port (channel 2), (f) data trace at the BAR port (channel 2), (g) eye diagram at the CROSS port (channel 2), (h) eye diagram at the BAR port (channel 2).

from the spectral response of the TM grating coupler stages that had a resonance dip around 1560nm. The multi-wavelength signal after exiting the receiver's pre-amplification stage (EDFA2) is depicted in Fig. 1(e). The wavelength-dependent gain profile of EDFA2 promoted the amplification of shorter wavelengths being closer to the peak spectral gain of the amplifier, leading in this way to different power levels and also different optical signal-to-noise ratios (OSNR) between the four received channels.

Experimental Results and Discussion
Fig. 2 illustrates representative data traces and eye diagrams for channel 1 (λ1) and channel 2 (λ2) signals recorded at the A-MZI CROSS and BAR output ports. The electrical control signal shown with the dashed curves had a repetition rate of 20KHz, with rectangular pulses of 15μs duration and an electric current peak value of 40mA. Successful operation of the device was obtained revealing inverted mode operation at the CROSS port with an ER value close to 14dB. The BAR output port had again a poor ER performance, not exceeding 0.9dB, due to the 95:5 coupler splitting ratio. The non-perfectly rectangular shape of the CROSS-port output data packets that yields an amplitude modulation of close to 1dB originates from the noise accumulated when being amplified in the receiver's stage amplifier units (EDFA2 and EDFA3), since the signal power emerging at the CROSS port was below the input power range requirements of the EDFA2 pre-amplifier. Similar results for both CROSS and BAR output ports were also obtained for data channels 3 and 4 at λ3 and λ4 wavelengths, respectively.

Fig. 3 presents the BER curves obtained for the four channels for the Back-to-Back (B2B) case and when the A-MZI operates in both ON and OFF operational states. Since the intention has been to monitor the signal degradation of the A-MZI device and not of the complete chip including its lossy in- and output grating coupler
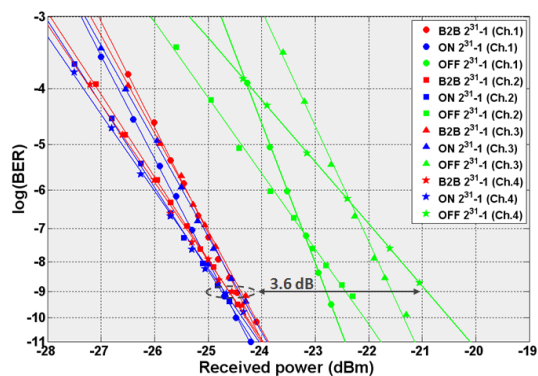
stages, a straight silicon waveguide employed on the chip has been used for the B2B case. During ON operation, the BER curve was recorded at the BAR output port controlling the A-MZI with a DC electric current value of 40mA. When operating in OFF state, the BER curve was obtained for the CROSS output port. In both ON and OFF operational states error-free performance was monitored. The ON state shows a negative power penalty close to the statistical error of 0.2dB for all four channels compared to the B2B curve. When operating at OFF state, the power penalties were ranging between 1.7dB and 3.6dB measured at a BER value of 10^{-9} for the four channels. The enhanced power penalty values compared to the corresponding ON state performance owes mainly to the 8dB lower power level received at MZI's CROSS output (-26dBm) against its BAR port during ON state (-18dBm). The power penalty increases with the channel wavelength, due to the wavelength-dependent gain and OSNR profile experienced by the four channels during amplification in EDFA2. Finally, the different slopes observed between the BER graphs of channels 1, 3 and the BER curves of channels 2 and 4 owe to the use of a separate data modulation stage per channel pair at the 4×10Gb/s transmitter end.

Conclusions
In conclusion, we have demonstrated the first active plasmonic device operating with true WDM traffic. An A-MZI switching structure employing silicon-based coupler stages and TO PMMA-based DLSPP waveguides as its active arms has been shown to provide error-free switching functionality with 4×10Gb/s incoming data traffic, requiring only 13.1mW of power and having response time in the μs scale. These results verify the potential of plasmonics in developing fast and low-power TO switches with small footprints for NoC environments.

Fig. 3: BER curves for all channels for B2B and during ON and OFF operational states.

References
[1] D. Van Thourhout et al., J. Sel. Top. Quant. Electron. **16**, 5 (2010).
[2] J. Gosciniak et al., Opt. Express **18**, 2 (2010).
[3] D. Kalavrouziotis et al., OFC'12, OW3E.3 (2012).
[4] K. Hassan et al., Appl. Phys. Lett. **99**, 241110 (2011).
[5] G. Giannoulis et al., IEEE PTL **24**, 5 (2011).